

Optimization electric field sensor sensitive electrodes of cylindrical form

S V Biryukov, S S Kolmogorova, A S Kolmogorov and D S Baranov

Omsk State Technical University, 11, Mira ave., Omsk, 644050, Russia

sbiryukov154@mail.ru

Abstract. The article researches into single-axis and two-axis electro-induction cylindrical sensors of electric field strength of various designs. The aim of the research in the article is to conduct a comparative analysis of these sensors from the point of view of the error in an inhomogeneous electric field with a high degree of heterogeneity and to identify their design parameters, the optimization of which could lead to a decrease in this error and the expansion of the spatial range of measurements. As a result of the study, the objective functions of the sensor error were obtained for the first time, which made it possible to optimize their design parameters and establish: 1) the optimal size of the sensitive electrode of the single-coordinate sensor is $\theta_0 = 53.5^\circ$, and the sensor error does not exceed $\pm 2\%$ in the entire spatial measurement range $0 \leq a < 1$; 2) two-coordinate sensors with the same error have only technically acceptable angular dimensions of the sensitive electrodes, respectively, for version 1 - $\theta_0 = 45^\circ$, for version 2 - $\theta_0 = 90^\circ$. The sensors in version 1 have a positive, and in version 2 a negative error in the spatial measurement range $0 \leq a < 0.25$, while the sensors in version 1 have a higher sensitivity. With approximately equal metrological characteristics, sensors with higher sensitivity should be selected. The practical goal of research is the possibility of sound design solutions to improve the metrological parameters of universal sensors used in electrometer devices for various purposes.

1. Introduction

The modern world pays great attention to assessing adverse influencing factors on technical, and especially biological, objects. One such factor is the low-frequency electromagnetic fields created by industrial facilities, such as power lines, electrical substations, railway contact networks, and others. In this regard, the market was flooded with means of measuring and monitoring low-frequency electric field strengths. An analysis of the instruments presented on the market showed that they are based on electric induction sensors of electric field strength of various designs [1-9], the error component of which is determining the entire measuring device.

Sensors can be structurally executed in the form of a disk (plate), cube, ball and cylinder — these are the most common forms of conductive bodies for constructing sensors of electric field strength [1, 9]. So [9] «in [3-6], spherical shape electric field sensors are considered and analyzed, in [6-8] - cubic and flat shape sensors». However, the metrological characteristics of the sensors presented on the instrument market are not confirmed by anything, and their error, according to the passport, is about 20% without indicating the spatial measurement range in which this error is provided.



2. Formulation of the problem

In this article, the authors posed and solved the following research tasks:

- 1) to consider and analyze the features of the construction and behavior of the sensor of electric field intensity of a cylindrical shape in fields of various inhomogeneities;
- 2) to identify the design parameters of cylindrical sensors responsible for their error and spatial range of measurements in electric fields of varying degrees of heterogeneity;
- 3) to compose the objective function, the optimization of which would allow to establish the optimal design parameters of the sensors, ensuring a decrease in their error and the expansion of the spatial range of measurement.

3. Theory

The optimization of the sizes of the sensitive elements of cylindrical electro-induction sensors reduces to obtaining the objective function linking the sizes of the sensitive elements of the sensor with its error in electric fields of various inhomogeneities.

As fields of various inhomogeneities, we choose a homogeneous electric field and a radial field of a linear charge with a strong degree of heterogeneity. A homogeneous field acts as a model, reference field. In relation to it, the error of the sensor operating in an inhomogeneous field of a linear charge will be estimated. We assume that the error of the sensor in other inhomogeneous fields is less than in the field of linear charge. By linear charge we mean an infinitely long uniformly charged thread. The linear charge field is selected from the condition of greatest inhomogeneity, which can be simulated by analyzing the behavior of the sensor in an inhomogeneous field [11].

To obtain the objective function, we will use the known relations of the electric charge density on the side surface of the conducting cylinder:

- in a homogeneous field [10]

$$\sigma = \sigma(\theta) = 2\varepsilon\varepsilon_0 E_0 \cdot \cos\theta \quad (1)$$

- in an inhomogeneous field of linear charge parallel to the axis of the cylinder [10]

$$\sigma = \sigma(\theta) = -\varepsilon\varepsilon_0 \frac{1}{a} \cdot \left[1 - \frac{(1-a^2)}{(1-2a\cos\theta+a^2)} \right] E_0, \quad (2)$$

where in formulas (1) and (2): ε is the dielectric constant of the environment; ε_0 is the dielectric constant; $a = R/d$ is a parameter characterizing the degree of field heterogeneity and determining the spatial range of measurement; R is the radius of the cylinder; d is the distance between the axis of symmetry of the cylinder and the axis of the linear charge; θ is the angle between the coordinate axis x and the position of the point on the side surface of the cylinder; E_0 is the intensity of the initial electric field before the introduction of a conducting cylinder into it.

The above relations (1) and (2) will allow us to determine the electric charges induced on the sensitive electrodes of the sensor and through them go to the target function that relates the error of the sensor to its geometric dimensions of the sensitive electrodes.

In consideration, one-coordinate [10] and two two-coordinate sensors [12] of electric field strength of various designs [13] will be involved.

Description of a single-axis cylindrical sensor [10]. “The sensor is based on a conductive cylinder 1 of radius R and height h . The cylinder can be either solid or hollow. On its side surface are diametrically opposite and isolated from each other and from the cylinder are two conductive sensitive electrodes 2 and 3 of a semicylindrical shape with an angular size of θ_0 and a concave part to the axis of the cylinder. The centers of the sensitive electrodes lie on the same coordinate axis. The maximum possible angular size θ_0 , which the sensing element can take, is $\pi/2$. Sensitive electrodes 2 and 3 are a thin conductive layer with a thickness of the order of $10 \div 100 \mu\text{m}$ deposited by nanotechnology methods on the surface of a conductive cylinder, and their radius and length coincide with the dimensions of the dielectric cylinder, as shown in Fig. 1.”

Assuming that the thickness of the sensitive electrodes and the distance from the cylindrical body of the sensor is much smaller than its radius R , we can assume that the sensitive electrodes 2 and 3 of the sensor have equal potentials (special measures will be taken for this), and the sensor is a single conducting cylindrical surface.

The presence of two diametrically sensitive electrodes 2 and 3 in the sensor allows it to be used as a double sensor in differential switching. Differential switching compensates in-phase components and increases the sensitivity of the sensor.

In [10], the author found differential electric charges induced on sensitive sensor electrodes
- in a homogeneous field

$$Q_{\text{dif}}^{\text{O}} = 8\varepsilon\varepsilon_0 R \cdot h \cdot \sin \theta_0 \cdot E_0; \quad (3)$$

- in an inhomogeneous field of linear charge parallel to the axis of the cylinder

$$Q_{\text{dif}}^{\text{H}} = 8\varepsilon\varepsilon_0 R \cdot h \cdot \left\{ \frac{1}{2a} \cdot \left[\arctan\left(\frac{1+a}{1-a} \tan \frac{\theta_0}{2}\right) - \arctan\left(\frac{1-a}{1+a} \tan \frac{\theta_0}{2}\right) \right] \right\} E_0 \quad (4)$$

where in formulas (3) and (4): α_0 is the angular size of the sensitive electrodes; h is the linear size of the sensitive electrodes; R is the radius of the sensitive electrode.

From the expressions (3) and (4) it follows that the differential sensitivities of the sensor in a homogeneous and inhomogeneous field are respectively equal:

$$G_{\text{dif}}^{\text{O}} = \frac{dQ}{dE_0} = 8\varepsilon\varepsilon_0 R \cdot h \cdot \sin \theta_0; \quad (5)$$

$$G_{\text{dif}}^{\text{H}} = \frac{dQ}{dE_0} = 8\varepsilon\varepsilon_0 R \cdot h \cdot \left\{ \frac{1}{2a} \cdot \left[\arctan\left(\frac{1+a}{1-a} \tan \frac{\theta_0}{2}\right) - \arctan\left(\frac{1-a}{1+a} \tan \frac{\theta_0}{2}\right) \right] \right\}. \quad (6)$$

An analysis of these sensitivities shows that the sensitivity of the sensor in a uniform field (5) is constant over the entire spatial range of existence of a uniform field. In contrast, the sensitivity of the

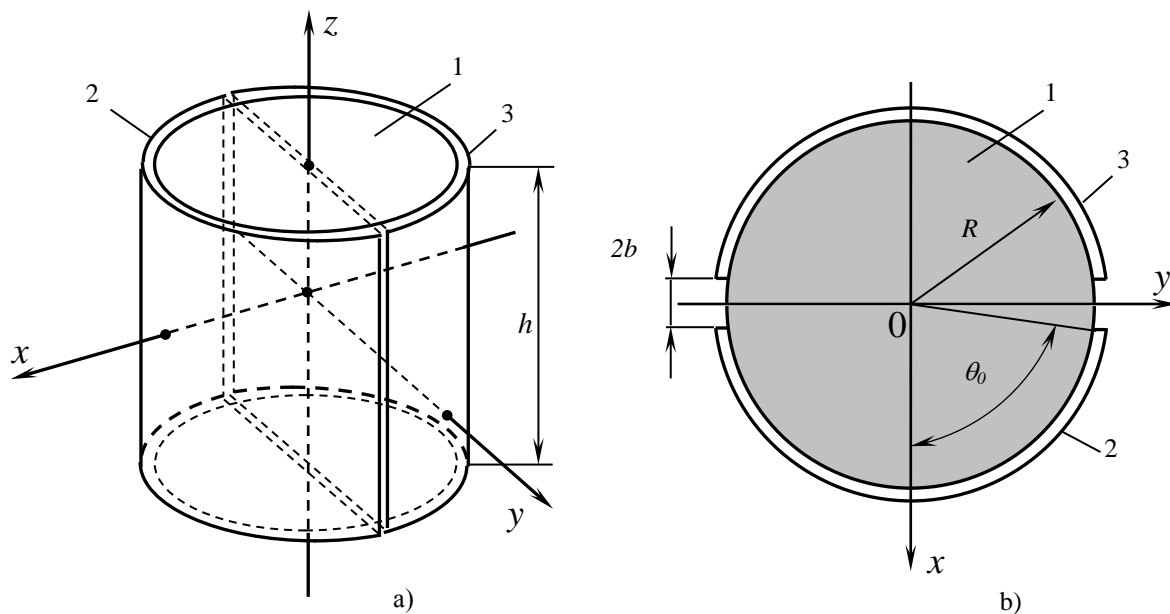


Figure 1. 3D view of a single-axis sensor (a), and a top view (b) [10]

sensor in an inhomogeneous field (6) depends on the parameter a , which determines the spatial

measurement range and indirectly characterizes the field inhomogeneity. The dependence of the sensitivity of the sensor on the spatial range of measurements will lead to additional error.

The obtained expressions (5) and (6) for the sensor sensitivities contribute to obtaining the objective function in the form of a relative sensitivity error from the degree of heterogeneity of the electric field, which makes it possible to optimize the angular dimensions of sensitive electrodes from the point of view of the minimum error and maximum spatial range of measurements.

The objective function in the form of relative error has the form [10]

$$\delta(a) = \frac{G_{dif}^H - G_{dif}^O}{G_{dif}^O} \times 100 = \left[\frac{\left[\arctan\left(\frac{1+a}{1-a} \tan\frac{\theta_0}{2}\right) - \arctan\left(\frac{1-a}{1+a} \tan\frac{\theta_0}{2}\right) \right]}{2a \cdot \sin\theta_0} - 1 \right] \times 100 \quad (7)$$

To optimize the sensitive electrodes of the sensor according to expression (7), we constructed the graphs of the objective error function presented in Fig. 2, a, b. In fig. Figure 2a shows the general course of the objective function for various angular sizes θ_0 of sensitive electrodes, depending on parameter a .

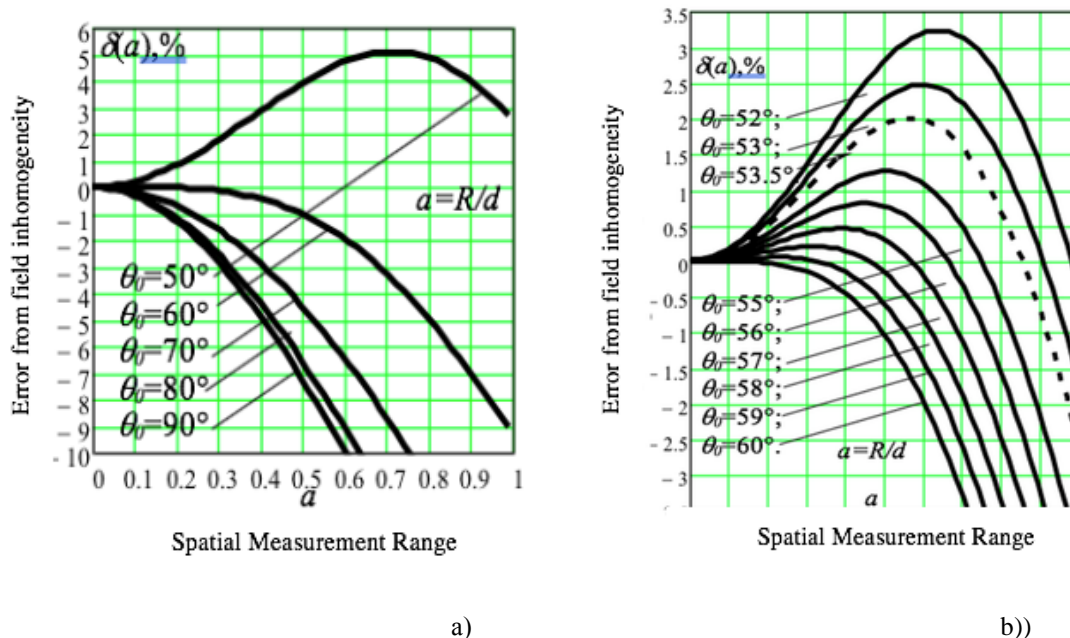


Figure 2. Graphs of the objective function of the error of the field inhomogeneity as a function of the parameter a and the angular dimensions of the sensitive electrodes α_0 a) the general course of the graphs; b) the progress of the graphs with the identification of the optimal size α_0 for the sensitive electrode.

It can be seen from the figure that a decrease in the angular size θ_0 of the sensitive electrode leads to a smooth transition of the sensor error from a region with a negative to a region with a positive error. This means that there are angular values θ_0 of the objective function for which the sensor error will be minimal in almost the entire spatial range determined by parameter a . Thus, Fig. 2a allows us to establish that the optimal angular dimensions of the sensitive electrodes lie in the range of θ_0 from 50° to 60° . In this regard, in this range, graphs of the objective function were constructed with a step of 1° , shown in Fig. 2, b.

From the graphs of fig. 2b it is seen (dashed curve) that from the point of view of the minimum error and the maximum spatial range of measurement, the optimal size of the sensitive electrodes is $\theta_0 = 53.5^\circ$. For this angular size of the sensitive electrode, the minimum possible error $\delta(a) = \pm 2\%$ lies in the maximum possible spatial range $0 < a < 0.99$. It should also be noted that any decrease in the angular

size of the sensitive electrode leads either to a decrease in the error in a given spatial range, or to an expansion of the spatial range of measurement at a given error.

Description of the two-axis cylindrical sensor. Two designs of a two-coordinate cylindrical sensor are possible. In the first version, four sensitive electrodes are formed by dissecting the cylinder by two mutually perpendicular planes passing through its axis of symmetry (Fig. 3, a) [12]. In the second, each of the four sensitive electrodes consists of a pair of elements formed by dissecting the cylinder by two mutually perpendicular planes passing through its axis of symmetry (Fig. 3b) [13].

In version 1, the sensor consists of a conducting cylinder 1 of radius R and height h (see Fig. 1). Conducting sensitive electrodes are arranged in pairs on the lateral surface of the cylinder on two coordinate axes x and y , diametrically opposite, isolated from each other and from the cylinder. A pair of electrodes 2 and 4 is diametrically opposite on the coordinate axis x , and a pair of electrodes 3 and 5 is located on the y axis. The electrodes are made in the form of cylindrical sectors with an angular size of θ_0 . The maximum possible angular size θ_0 , which the sensitive electrode can take, is $\pi/4$. All requirements and assumptions for a two-axis sensor are similar to the requirements for a single-axis sensor. The top view of the sensor and its location in the electric field is shown in Fig. 3, a.

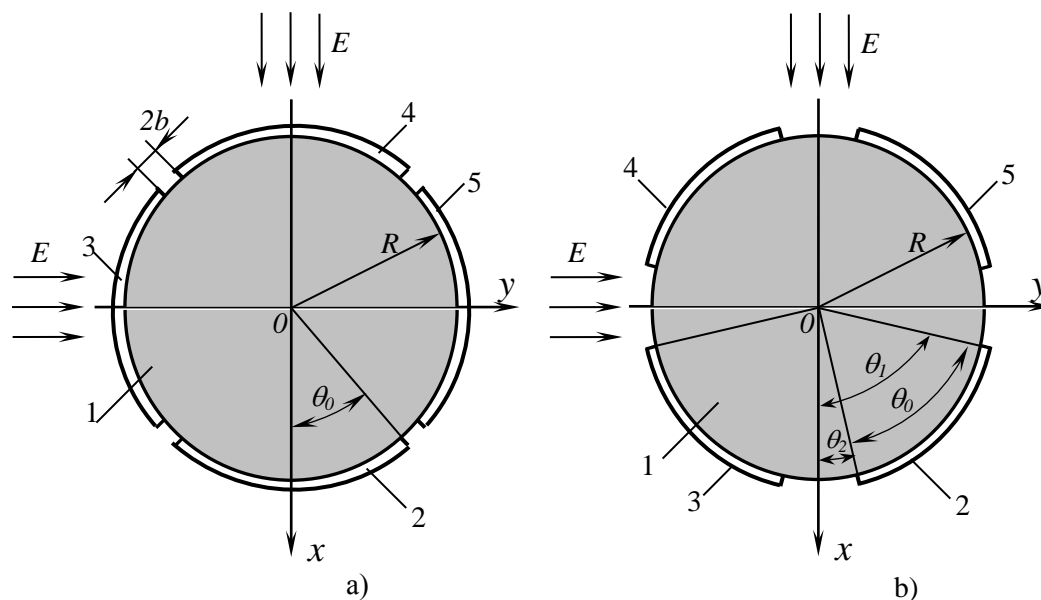


Figure 3. Two-coordinate sensors of various design, top view: a) with sensitive electrodes in the form of a cylindrical sector; b) with compound sensitive electrodes

Expressions (3) and (4) for differential charges and expressions (4) and (5) for differential sensitivities are valid for the sensor.

Using formulas (3) and (4), we write down the expressions for the differential charges of the two-coordinate sensor corresponding to the coordinate axes x and y

– in a homogeneous field

$$Q_{\text{dif},x}^0 = 8\varepsilon\varepsilon_0 R \cdot h \cdot \sin \theta_0 \cdot E_x; \quad (8)$$

$$Q_{\text{dif},y}^0 = 8\varepsilon\varepsilon_0 R \cdot h \cdot \sin \theta_0 \cdot E_y.$$

– in an inhomogeneous field of linear charge parallel to the axis of the cylinder

$$\begin{aligned}
 Q_{\text{dif},x}^{\text{H}} &= 8\varepsilon\varepsilon_0 R \cdot h \cdot \left\{ \frac{1}{2a} \cdot \left[\arctan\left(\frac{1+a}{1-a} \tan \frac{\theta_0}{2}\right) - \arctan\left(\frac{1-a}{1+a} \tan \frac{\theta_0}{2}\right) \right] \right\} E_x; \\
 Q_{\text{dif},y}^{\text{H}} &= 8\varepsilon\varepsilon_0 R \cdot h \cdot \left\{ \frac{1}{2a} \cdot \left[\arctan\left(\frac{1+a}{1-a} \tan \frac{\theta_0}{2}\right) - \arctan\left(\frac{1-a}{1+a} \tan \frac{\theta_0}{2}\right) \right] \right\} E_y.
 \end{aligned}
 \tag{9}$$

where in formulas (8) and (9):

$$E_x = E_0 \cos \alpha; \quad E_y = E_0 \cos \beta, \tag{10}$$

where α and β are the direction cosines between the vector and the coordinate axes x and y of the sensor, respectively, for which the condition

$$\cos^2 \alpha + \cos^2 \beta = 1. \tag{11}$$

Thus, E_x and E_y are the projections of the vector E_0 on the coordinate axes x and y .

With this in mind and substituting expressions (10) into expressions (8) and (9), the total electric charge forming the output signal of the two-coordinate sensor will be

– in a homogeneous field

$$Q^{\text{O}} = \sqrt{(Q_{\text{dif},x}^{\text{O}})^2 + (Q_{\text{dif},y}^{\text{O}})^2} = 8\varepsilon\varepsilon_0 R \cdot h \cdot \sin \theta_0 \cdot E_0. \tag{12}$$

– in an inhomogeneous field of linear charge parallel to the axis of the cylinder

$$\begin{aligned}
 Q^{\text{H}} &= \sqrt{(Q_{\text{dif},x}^{\text{H}})^2 + (Q_{\text{dif},y}^{\text{H}})^2} = \\
 &= 8\varepsilon\varepsilon_0 R \cdot h \cdot \left\{ \frac{1}{2a} \cdot \left[\arctan\left(\frac{1+a}{1-a} \tan \frac{\theta_0}{2}\right) - \arctan\left(\frac{1-a}{1+a} \tan \frac{\theta_0}{2}\right) \right] \right\} E_0.
 \end{aligned}
 \tag{13}$$

Then the total sensitivities of the two-coordinate sensor in a homogeneous and inhomogeneous field will be respectively equal to:

$$G_{\text{dif}}^{\text{O}} = \frac{dQ}{dE_0} = 8\varepsilon\varepsilon_0 R \cdot h \cdot \sin \theta_0; \tag{14}$$

$$G_{\text{dif}}^{\text{H}} = \frac{dQ}{dE_0} = 8\varepsilon\varepsilon_0 R \cdot h \cdot \left\{ \frac{1}{2a} \cdot \left[\arctan\left(\frac{1+a}{1-a} \tan \frac{\theta_0}{2}\right) - \arctan\left(\frac{1-a}{1+a} \tan \frac{\theta_0}{2}\right) \right] \right\}, \tag{15}$$

and coincide with similar expressions (5) and (6) for a single-axis sensor. In this case, the objective function in the form of relative error will coincide with the similar function (7) for the single-axis sensor.

As noted above for a single-axis sensor, the sensitivity of a two-coordinate sensor also in an inhomogeneous field does not remain constant, but depends on the distance to the field source, which leads to an additional error of the sensor from the inhomogeneity of the electric field. For the considered design of the two-coordinate sensor, this error will be determined by expression (7), only the limiting angular size of the sensitive electrode should be selected from the range $\theta_0 \leq \pi/4$.

We will optimize the sensitive electrodes of the two-coordinate sensor based on expression (7). For this, using the mathematical editor of MathCAD 14, we construct graphs of the objective error function (fig. 4).

From fig. 4 it follows that the only optimal angular size of the sensitive electrode is the size determined by the angle $\theta_0 = 45^\circ$. The error graph corresponding to this angular size of the sensitive electrode in almost the entire spatial measurement range $0 < a < 1$ does not go beyond +12%. The same graph should be used when choosing a smaller sensor error and establishing a limited spatial measurement range for it. So, for example, from the graph of Fig. 4 it follows that for the error $\delta = 3\%$ the spatial range will not exceed $a \leq 0.3$.

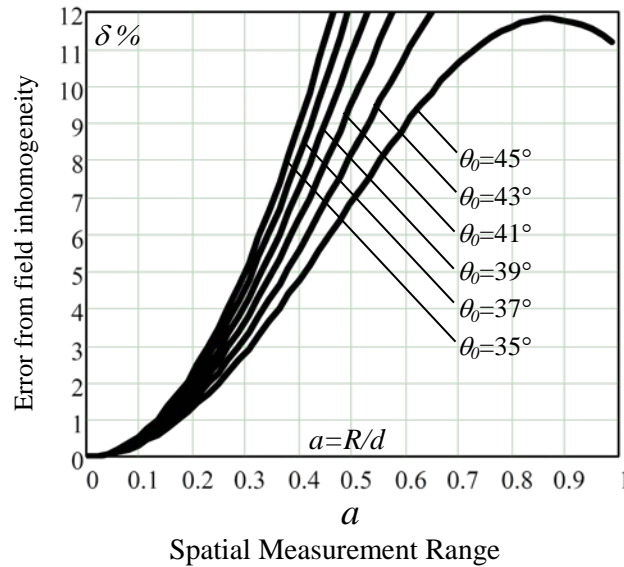


Figure 4. Graphs of the objective function of the error of the field inhomogeneity as a function of parameter a for given angular dimensions of the sensitive electrodes θ_0

In version 2, the sensor also consists of a conducting cylinder 1 of radius R and height h (see Fig. 1). On the lateral surface of the cylinder on two coordinate axes x and y are diametrically opposite, isolated from each other and from the cylinder, conductive sensitive electrodes of equal size are arranged in pairs, as shown in Fig. 3, b. Each sensitive electrode consists of two sensitive elements. So on the x -axis, two pairs of sensors 2, 3 and 4, 5 are diametrically opposed, and on the y -axis are two pairs of sensors 2, 5 and 3, 4. The sensitive electrodes are made in the form of cylindrical sectors limited by angular dimensions θ_1 and θ_2 (see Fig. 3, b). Thus, each sensitive element is limited by the angular size $\theta_0 = \theta_1 - \theta_2$. The maximum possible angular size is $\theta_0 = \pi/2$ for $\theta_1 = \pi/2$ and $\theta_2 = 0$, and the minimum possible $\theta_0 = 0$ for $\theta_1 = \pi/4$ and $\theta_2 = \pi/4$. All requirements and assumptions for this sensor are similar to the requirements for the above sensors.

In the sensor under consideration, the sensitive electrode differs from the sensitive electrode of the single-coordinate sensor in that a cylindrical segment with an angular size of θ_2 is cut out from the middle part of the electrode with an external angular size of θ_1 corresponding to the angular size of θ_0 of the single-coordinate sensor. Based on the foregoing and expressions (3) and (4), we write the expressions for the differential charges of the two-coordinate sensor corresponding to the coordinate axes x and y

- in a homogeneous field

$$Q_{\text{dif.x}}^o = 8\epsilon\epsilon_0 R \cdot h \cdot (\sin \theta_1 - \sin \theta_2) E_x; \tag{16}$$

$$Q_{\text{dif.y}}^o = 8\epsilon\epsilon_0 R \cdot h \cdot (\sin \theta_1 - \sin \theta_2) E_y. \tag{17}$$

- in an inhomogeneous field of linear charge parallel to the axis of the cylinder

$$Q_{\text{dif.x}}^H = 8\epsilon\epsilon_0 R \cdot h \cdot \left\{ \frac{1}{2a} \cdot \left[\left[\arctan\left(\frac{1+a}{1-a} \tan \frac{\theta_1}{2}\right) - \arctan\left(\frac{1-a}{1+a} \tan \frac{\theta_1}{2}\right) \right] - \left[\arctan\left(\frac{1+a}{1-a} \tan \frac{\theta_2}{2}\right) - \arctan\left(\frac{1-a}{1+a} \tan \frac{\theta_2}{2}\right) \right] \right] \right\} E_x; \tag{18}$$

$$Q_{\text{dif.y}}^H = 8\epsilon\epsilon_0 R \cdot h \cdot \left\{ \frac{1}{2a} \cdot \left[\left[\arctan\left(\frac{1+a}{1-a} \tan \frac{\theta_1}{2}\right) - \arctan\left(\frac{1-a}{1+a} \tan \frac{\theta_1}{2}\right) \right] - \left[\arctan\left(\frac{1+a}{1-a} \tan \frac{\theta_2}{2}\right) - \arctan\left(\frac{1-a}{1+a} \tan \frac{\theta_2}{2}\right) \right] \right] \right\} E_y, \tag{19}$$

Given the substitution of expressions (10), (11) in expressions (16), (17), (18) and (19), the total electric charge forming the output signal of the two-coordinate sensor will be

– in a homogeneous field

$$Q^O = \sqrt{(Q_{\text{dif.x}}^O)^2 + (Q_{\text{dif.y}}^O)^2} = 8\epsilon\epsilon_0 R \cdot h \cdot (\sin \theta_1 - \sin \theta_2) \cdot E_0 = 8\sqrt{2}\epsilon\epsilon_0 R \cdot h \cdot \sin \frac{\theta_0}{2} E_0. \tag{20}$$

– in an inhomogeneous field of linear charge parallel to the axis of the cylinder

$$Q^H = \sqrt{(Q_{\text{dif.x}}^H)^2 + (Q_{\text{dif.y}}^H)^2} = 8\epsilon\epsilon_0 R \cdot h \cdot \left\{ \frac{1}{2a} \cdot \left[\left[\arctan\left(\frac{1+a}{1-a} \tan \frac{\theta_1}{2}\right) - \arctan\left(\frac{1-a}{1+a} \tan \frac{\theta_1}{2}\right) \right] - \left[\arctan\left(\frac{1+a}{1-a} \tan \frac{\theta_2}{2}\right) - \arctan\left(\frac{1-a}{1+a} \tan \frac{\theta_2}{2}\right) \right] \right] \right\} E_0. \tag{21}$$

Then the total sensitivities of the two-coordinate sensor in a homogeneous and inhomogeneous field will be respectively equal to:

$$= \dots = \left(\dots \right) = \sqrt{\dots} \dots; \tag{22}$$

$$G_{\text{dif.}}^H = \frac{dQ}{dE_0} = 8\epsilon\epsilon_0 R \cdot h \cdot \left\{ \frac{1}{2a} \cdot \left[\left[\arctan\left(\frac{1+a}{1-a} \tan \frac{\theta_1}{2}\right) - \arctan\left(\frac{1-a}{1+a} \tan \frac{\theta_1}{2}\right) \right] - \left[\arctan\left(\frac{1+a}{1-a} \tan \frac{\theta_2}{2}\right) - \arctan\left(\frac{1-a}{1+a} \tan \frac{\theta_2}{2}\right) \right] \right] \right\}. \tag{23}$$

Expressions (22) and (23) make it possible to obtain the objective function in the form of a relative error [9] of sensitivity from inhomogeneity of the electric field:

$$\delta(a) = \frac{G_{\text{dif.}}^H - G_{\text{dif.}}^O}{G_{\text{dif.}}^O} \times 100 = \left[\frac{\arctan\left(\frac{1+a}{1-a} \tan \frac{\theta_1}{2}\right) - \arctan\left(\frac{1-a}{1+a} \tan \frac{\theta_1}{2}\right) - \arctan\left(\frac{1+a}{1-a} \tan \frac{\theta_2}{2}\right) + \arctan\left(\frac{1-a}{1+a} \tan \frac{\theta_2}{2}\right)}{2a \cdot (\sin \theta_1 - \sin \theta_2)} - 1 \right] \times 100 \tag{24}$$

We plot the objective error function according to expression (24), and optimize the angular dimensions of the sensor’s sensitive electrodes from the point of view of the minimum error and maximum spatial measurement range. Error plots for different angular sizes θ_1 and θ_2 of sensitive electrodes are presented in Fig. 5.

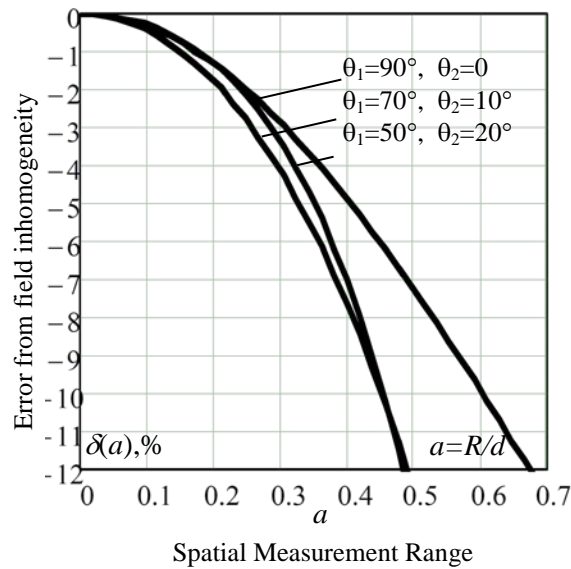


Figure 5. Graphs of the objective function of the error of the field inhomogeneity versus parameter a for given angular sizes of the sensitive electrodes θ_1 and θ_2 .

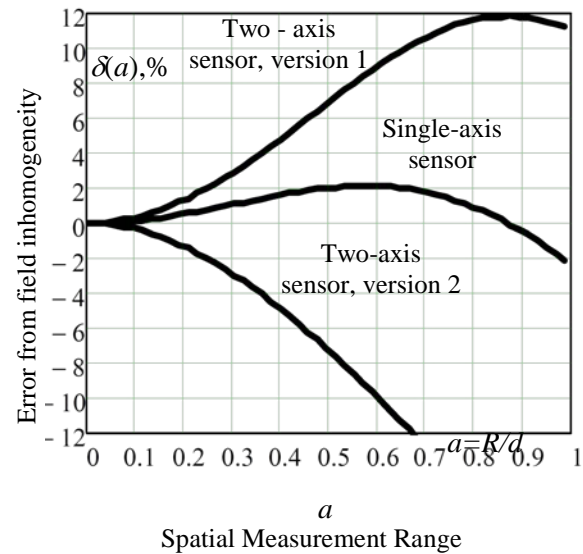


Figure 6. Graphs of the objective error function for the optimal and technically acceptable angular dimensions of the sensitive electrodes of the three

It follows from the figure that the graphs lie in the negative region of the error and decrease monotonously. In this regard, the two-coordinate sensor in the second version does not have optimal angular dimensions of the sensitive electrodes. Therefore, the best technical solution in this situation according to Fig. 5 will be the choice of the angular size of the sensitive electrodes, which corresponds to the error curve with $\theta_1 = 90^\circ$ and $\theta_2 = 0$, in this case $\theta_0 = \theta_1 - \theta_2 = 90^\circ$. These angular dimensions of the sensitive electrodes correspond to the error graph with the widest spatial measurement range $0 < a < 0.67$ within the error range from 0 to +12%. The same graph should be followed when choosing a smaller sensor error, and establishing a limited spatial measurement range for it. So, for example, from the graph of Fig. 5 it follows that for the error $\delta = 3\%$ the spatial range will not exceed $a \leq 0.3$.

The last stage of the research is to compare the relative sensitivities (Table 1) and the graphs of the objective error function for the optimal and technically acceptable angular sizes of the sensitive electrodes of the single-coordinate and two-coordinate sensors in versions 1 and 2 (Fig. 6).

Table 1.

	Single-axis sensor	Two-axis sensor, version 1	Two-axis sensor, version 2
θ_0	53.5°	45°	90°
G	$G_{\text{dif}}^0 1 = 8\epsilon\epsilon_0 R \cdot h \cdot \sin \theta_0$	$G_{\text{dif}}^0 2 = 8\epsilon\epsilon_0 R \cdot h \cdot \sin \theta_0$	$G_{\text{dif}}^0 3 = 8\sqrt{2}\epsilon\epsilon_0 R \cdot h \cdot \sin \frac{\theta_0}{2}$
$\frac{G}{G_{\text{dif}}^0 1}$	1	0.88	1.24

From the table 1 shows that the two-coordinate sensor in version 2 has a greater sensitivity than the sensor in version 1 with respect to the sensitivity of a single-axis sensor.

Comparison of graphs Fig. 6 show that a single-axis cylindrical sensor has a minimum error of $\pm 2\%$ in almost the entire spatial measurement range $0 \leq a < 1$. Two-coordinate cylindrical sensors have the same, but different in sign errors (positive - execution 1, negative - execution 2) in a smaller spatial measurement range $a \leq 0.25$. For the sensor in the first version, the error will be $\pm 12\%$ with the maximum possible spatial range $0 \leq a < 1$, and for the sensor in the second version, the error $\pm 12\%$ will be in the spatial range $0 \leq a < 0.67$.

4. Results

The optimization of the angular dimensions of the sensitive electrodes of cylindrical sensors showed that the optimal size of the sensitive electrode is possible only for a single-axis sensor and is $\theta_0 = 53.5^\circ$. With such an angular size of the sensor's sensitive electrode, the error will not exceed $\pm 2\%$ in the spatial measurement range $0 \leq a < 1$. Two-coordinate sensors have only technically acceptable angular dimensions of the sensitive electrodes, which are: a) for version 1 - $\theta_0 = 45^\circ$; b) for execution 2 - $\theta_0 = 90^\circ$. For two-coordinate sensors of the indicated angular dimensions of the sensitive electrode, the sensor error in version 1 is positive, and in version 2 it is negative in the entire spatial measurement range and already for $a > 0.3$ goes beyond $\pm 3\%$. In this regard, a single-coordinate sensor is suitable for measuring in the entire spatial range of measurement with an error of $\pm 2\%$, and two-coordinate sensors with the same error are suitable for measuring at distances from the field source d equal to four radii of the cylindrical body of the sensor ($d = 4R$). When choosing a sensor, you should pay attention to its sensitivity. So, two-coordinate sensors in version 2 have a high sensitivity. Therefore, with approximately equal metrological characteristics, sensors with higher sensitivity should be selected.

5. Conclusions

For the first time, the problem of optimizing the angular dimensions of sensitive electrodes of cylindrical sensors of electric field strength was solved. For this purpose, the objective functions (7) for the single-axis and two-axis sensors in version 1 and (24) for the two-axis sensors in version 2 were obtained. The objective functions are presented in the form of a relative error in the sensitivity of the sensors from the degree of heterogeneity of the electric field and allow optimization of the angular dimensions of the sensitive electrodes of the sensors from the point of view of the minimum error δ and the maximum of the spatial range of measurements $a = R / d$. The analysis of the graphical dependencies of the objective error functions (Fig. 2, Fig. 4 and Fig. 5) shows that the sensors considered are suitable for measuring the electric field strength. Single-axis sensors can be used in the spatial measurement range $0 \leq a < 1$ with an error of $\pm 2\%$ with an optimal angular size of the sensitive electrode $\theta_0 = 53.5^\circ$. The two-coordinate sensors in version 1 can be used in the spatial measurement range $0 \leq a < 1$ with an error of $+ 12\%$ at the optimal angular size of the sensitive electrode $\theta_0 = 45^\circ$, and in version 2 - in the spatial measurement range $0 \leq a < 0.67$ with the same, but with a negative error of 12% at the optimal angular size of the sensitive electrode $\theta_0 = 90^\circ$. The errors of the two-coordinate sensors can be minimized to the desired extent by reducing the spatial measurement range.

References

- [1] Kolmogorova S S, Kolmogorov A S and Biryukov S V 2018 *The modern presentation of sensors of electromagnetic fields, measuring instruments based on them and applications in various operating conditions* (Scientists of Omsk - to the region: materials III Region. scientific and technical conf. Omsk, 6-7 June) pp 11–16
- [2] Biryukov S V and Tyukin A V *Design errors of three-coordinate sensors of electric field strength* (Omsk Scientific Herald. 2017 No 3 (153) p 82–86
- [3] Feser K A and Paff W 1984 *Potential free spherical sensor for the measurement of transient electric fields* (IEEE Transaction on Power Apparatus and Systems, vol. Pas-103 No 10) p 2904–2911
- [4] Horvath T 1979 *Measurement of the distortion less electric field intensity of high voltage*

- installations* (Third International Symposium on High voltage Engineering. Milan, 28-31 Aug) p. 44.05
- [5] Bassen H I and Smith G S 1983 *Electric field probes - a review* (IEEE Transactions on Antennas and Propagation vol AP-31 No 5) pp 710-718
- [6] Biryukov S V 2000 *The theory and practice of constructing electric induction sensors of potential and electric field strength* (Omsk Scientific Bulletin vol. 11) p 89-93.
- [7] Gatman S 1968 *Dual electric field meter with protection* (Instruments for scientific research No. 1) pp 45-49
- [8] Biryukov S V and Shchapova L V 2017 *The electric field intensity sensor in the form of a flat conductive plate in the form of a square* (Omsk Scientific Bulletin No 5 (155) p 126-130.
- [9] Biryukov S V and Korolyova M A 2017 *Electroinduction disk sensor of electric field strength* (IOP Conf. Series: Journal of Physics: Conf Series vol 944) p 012017-1 – 012017-8. DOI: 10.1088 / 1742-6596 / 944/1/012017
- [10] Biryukov S V, Baranov D S, Kolmogorova S S and Tyukin A V 2017 *Electric field strength sensor of cylindrical form* (IOP Conf. Series: Journal of Physics: Conf Series 944, conf.1. 012017) p 8 DOI: 10.1088 / 1742-6596 / 944/1/012017
- [11] Biryukov S V, Kolmogorov A S and Kolmogorova S S 2018 *Interaction of the conductive surface of a cylindrical sensor with an electric field of a uniformly charged straight-line thread parallel to the axis of the cylinder* (Omsk Scientific Bulletin No 3 (159) pp 18–21
- [12] Klimashevsky I P Kondratiev B L, Poletaev V A and Yurkevich V M 1983 *An electric field vector meter of high-voltage equipment* (Measuring equipment No 1) pp 48–49
- [13] Biryukov S V and Blesman A I 2018 *Utility Model Patent* (Russian Federation No. 183095 IPC G01R29/12 / - No. 2018120984; Stated 06.06.2018; Publ. 09/11/2018, Bull. Number 26)
- [14] 王平 2016 *High density electrical measurement device and its method to measure polarizability through the use of metal electrodes*. (CN106501864A; filed Nov. 08, 2016; published March 15, 2017)
- [15] Jack Y Dea 2011 *Chopperless ambient electric field sensor* (United States Patent US8653822B1; filed Feb. 18, 2011; published Feb. 18, 2014)